DIFFRACTION OF NORMAL SH-WAVE FROM A SEMI-INFINITE RIGID INCLUSION IN AN ELASTIC LAYER

M. V. Voytko, Ya. P. Kulynych

Karpenko Physico-Mechanical Institute of the NAS of Ukraine, Lviv

E-mail: myron.voytko@gmail.com

The Fourier integral transform is used to reduce the diffraction problem of the normal SH-wave on a semi-infinite rigid inclusion in elastic layer to the Wiener–Hopf equation. Its solution is obtained by the factorization method. The analytical expressions of the diffracted displacement fields are represented in any region of interest. The dependences of the scattered field on the parameters of the structure are given. The properties of identification of the inclusion type defect in the plane layer are illustrated.

Keywords: *elastic layer, inclusion, diffraction, normal SH-wave, Wiener–Hopf technique.*

ДИФРАКЦІЯ НОРМАЛЬНОЇ SH-ХВИЛІ НА НАПІВНЕСКІНЧЕННОМУ ЖОРСТКОМУ ВКЛЮЧЕННІ В ПРУЖНОМУ ШАРІ

М. В. Войтко, Я. П. Кулинич

Фізико-механічний інститут ім. Г. В. Карпенка НАН України, Львів

Досліджено дифракцію нормальної SH-хвилі на напівнескінченному жорсткому вклю-ченні, розташованому несиметрично відносно плоских поверхонь пружного шару. Вва-жали, що поверхні шару вільні від напружень. Включення моделювали півплощиною, на якій зміщення рівні нулю. Задачу зведено до змішаної крайової задачі для рівняння Гельм-гольца, розв'язок якої повинен задовольняти умови Діріхле на дефекті, Неймана на по-верхнях шару, а також випромінювання на нескінченності і Мейкснера на вершинах де-фекту. Використовуючи інтегральне перетворення Фур'є, змішану крайову задачу звели до функціонального рівняння Вінера–Гопфа, яке є справедливим у визначеній смузі регу-лярності. Для розв'язання цього рівняння використано метод декомпозиції та теорему Ліувіля. Для цього спочатку факторизовано характеристичну функцію. Вона подана у вигляді добутку двох функцій, які є регулярними у півплощинах і мають спільну смугу регулярності. За межами областей регулярності ці функції допускають особливості типу простих полюсів. Розв'язок рівняння Вінера–Гопфа подано в аналітичному вигляді. Далі, застосовуючи обернене перетворення Фур'є, знайшли вирази для розсіяних полів змі-щень у кожній із підобластей для довільної частоти і точки простору. Наведено графіки залежностей дифрагованого поля зміщень на поверхнях шару залежно від координати, положення дефекту та частоти зондування. Проілюстровано ознаки для ідентифікації дефекту типу включення в плоскому шарі. Встановлено товщину шару та частоти його зондування основною хвилевідною модою, за яких місце формування інтенсивних осци-ляцій пружного поля на поверхнях є ознакою утворення краю дефекту, який простягаєть-ся в область, де осциляції відсутні. Зміна частотного параметра (підвищення частоти) дає змогу оцінити глибину його залягання.

Ключові слова: *пружний шар, включення, дифракція, нормальна SH-хвиля, метод Вінера–Гопфа.*

Introduction. The study of the diffraction of elastic waves by defects located in various constructions is important for the development of new intelligent diagnostic technologies that combine the usage of various technical means for collecting and processing the information. For example, they are based on the common use of optical and ultrasonic methods [1–6]. In order to provide the theoretical basis for this techno-logy, the problem of SH-wave diffraction from a finite crack in an elastic layer and on a crack located at the boundary of the junction of a layer with a half-space is solved by the Wiener–Hopf technique [7–11]. In this paper, the cracks are modelled by a finite slit of zero thickness without any stresses on the faces. Within the framework of this model, the

resonance vibrations are analyzed to obtain the maximum response. The problem of SH-wave scattering from a semi-infinite crack in a plane elastic waveguide is solved by the mode-matching technique [12]; the reflected and transmitted coefficients as functions of frequency are analyzed.

The purpose of this paper is to model the displacement field on the layer surfaces with an internal defect for its further identification. For this purpose, the problem of SH-wave diffraction from the defect located in the elastic layer is solved. The defect is modelled by the rigid semi-infinite inclusion of zero thickness. Time factor is assumed to be $e^{-i\omega t}$ and omitted throughout the paper.

Fig. 1. Geometrical scheme of the problem.

Formulation of the problem. Let us consider the elastic layer in the Cartesian coordinate system xOy

$$P(y):\left\{x\in\left(-\infty,+\infty\right),\ y\in\left(-d,+d\right),\ z\in\left(-\infty,+\infty\right)\right\}$$

with the rigid inclusion (Fig. 1):

$$\Gamma(h):\left\{x\in\left(-\infty,0\right),\ y=h,z\in\left(-\infty,+\infty\right)\right\}.$$

Let the incident normal transverse elastic wave of the horizontal polarization (SH-wave) propagates in the negative direction of the axis x as

$$u_z^{inc}\left(x,y\right)=e^{\gamma_j x}\cos\left(\beta_j y\right),\tag{1}$$

where $\beta_j=\dfrac{\pi j}{2d}$, $\gamma_j=\sqrt{\beta_j^2-k^2}$, $j=0,2,\dots$; k is the wave number, $k=k'+ik''$, $k',k''>0$.

We seek the unknown diffracted field $u=u(x,y)$ from the solution of the mixed boundary value problem for Helmholtz equation

$$\partial_x^2 u\left(x,y\right)+\partial_y^2 u\left(x,y\right)+k^2 u\left(x,y\right)=0,\tag{2}$$

with the boundary conditions on the defect

$$u^{tot}\left(x,h\pm0\right)=0,\quad x\in\left(-\infty,0\right)\tag{3}$$

and on the elastic layer surfaces

$$\partial_y u^{tot}\left(x,y=\pm d\right)=0,\quad x\in\left(-\infty,+\infty\right),$$

where $u^{tot}=u+u^{inc}$ is the total field. We seek the solution in the class of functions which satisfy the radiation and the edge conditions.

Solution of the problem. Let us introduce the Fourier integral transformation of the diffracted field as follows

$$U\left(\alpha,y\right)=\frac{1}{\sqrt{2\pi}}\int_{-\infty}^{+\infty}u\left(x,y\right)e^{i\alpha x}dx,\tag{4}$$

where $\alpha=\sigma+i\tau$ (σ, τ are the real values).

Next, we represent the solution of equation (2) in the Fourier transform domain in the form

$$U(\alpha, y) = \begin{cases} A(\alpha)e^{\gamma y} + B(\alpha)e^{-\gamma y}, & h < y < d, \\ C(\alpha)e^{\gamma y} + D(\alpha)e^{-\gamma y}, & -d < y < h. \end{cases} \tag{5}$$

Here, $A(\alpha)$, $B(\alpha)$, $C(\alpha)$, $D(\alpha)$ are unknown functions, that are regular in the strip $\alpha \in \Pi$: $\{-\tau_0 < \tau < \tau_0\}$, where $k'' < \tau_0 < k'$; in order to satisfy the radiation condition at infinity, we find that $\operatorname{Re}\gamma > 0$, where $\gamma = \sqrt{\alpha^2 - k^2}$.

Let us introduce the Fourier integrals:

$$U^-(\alpha, h \pm 0) = \frac{1}{\sqrt{2\pi}} \int_{-\infty}^{0} u(x, h \pm 0)e^{i\alpha x}dx, \tag{6}$$

$$U^+(\alpha, h \pm 0) = \frac{1}{\sqrt{2\pi}} \int_{0}^{+\infty} u(x, h \pm 0)e^{i\alpha x}dx. \tag{7}$$

Here, $U^-(\alpha, h \pm 0)$, $U^+(\alpha, h \pm 0)$ are regular functions in the overlapping half-planes $\tau < \tau_0$, $\tau > -\tau_0$ with a common strip of regularity $\alpha \in \Pi$.

Applying the Fourier transform to the boundary condition (3), we find that

$$U^-(\alpha, h + 0) = U^-(\alpha, h - 0) = U^-(\alpha)$$

and

$$U^-(\alpha) = \frac{i\cos(\beta_j h)}{\sqrt{2\pi}(\alpha - i\gamma_j)}. \tag{8}$$

Using notations (6)–(8), we rewrite the expression (5) as follows:

$$U(\alpha, y) = \begin{cases} \dfrac{U^-(\alpha) + U^+(\alpha)}{\operatorname{ch}(\gamma(h - d))} \operatorname{ch}(\gamma(y - d)), & h < y < d, \\ \dfrac{U^-(\alpha) + U^+(\alpha)}{\operatorname{ch}(\gamma(h + d))} \operatorname{ch}(\gamma(y + d)), & -d < y < h. \end{cases} \tag{9}$$

Further, using the condition of continuity of the normal stresses at $\{x \in (0, +\infty), y = h \pm 0\}$, we reduce the problem to the Wiener–Hopf equation [13, 14]:

$$U^+(\alpha)M_+(\alpha) + \frac{i\cos(\beta_j h)M_+(\alpha)}{\sqrt{2\pi}(\alpha - i\gamma_j)} = \frac{J_1^-(\alpha)}{M_-(\alpha)}, \quad \alpha \in \Pi. \tag{10}$$

Here, $J_1^-(\alpha) = \dfrac{1}{\sqrt{2\pi}} \int_{-\infty}^{0} \left[\partial_y u(x, h + 0) - \partial_y u(x, h - 0)\right]e^{i\alpha x}dx$ is the unknown function that is regular in the lower half-plane $\tau < \tau_0$; $U^+(\alpha) = O\left(\alpha^{-3/2}\right)$, $J_1^-(\alpha) = O\left(\alpha^{-1/2}\right)$, if $|\alpha| \mapsto \infty$ in the domain of regularity. The known functions $M_-(\alpha)$, $M_+(\alpha)$ are regular in overlapping half-planes $\tau < \tau_0$, $\tau > -\tau_0$, respectively. Outside the strip Π they have simple zeros at $\alpha = \pm i\gamma_{n1}$ and poles at $\alpha = \pm i\gamma_{n2}$, $\alpha = \pm i\gamma_{n3}$, $n = 1, 2, \dots$,

where

$$\gamma_{n1} = \frac{1}{2d}\sqrt{(\pi n)^2 - (2kd)^2} \ ,$$

$$\gamma_{n2} = \frac{1}{l_1}\sqrt{\left(\pi\left(n - \frac{1}{2}\right)\right)^2 - (kl_1)^2} \ ,$$

$$\gamma_{n3} = \frac{1}{l_2}\sqrt{\left(\pi\left(n - \frac{1}{2}\right)\right)^2 - (kl_2)^2} \ ,$$

$$l_{1(2)} = d \mp h \ ;$$

$$M_+(\alpha) = M_-(-\alpha) \quad \text{and} \quad M_\pm(\alpha) = O(\alpha^{1/2}), \ \text{if} \ |\alpha| \mapsto \infty \ ;$$

$$M_+(\alpha) = \sqrt{2d} \ \frac{-ie^{\chi(\alpha)}(\alpha + k)\sqrt{\sin(2kd)}\,M_1(\alpha)}{\Lambda\,M_2(\alpha)M_3(\alpha)} \ , \qquad (11)$$

$$\chi(\alpha) = -\frac{i\alpha}{\pi\left(l_1\ln\left(\dfrac{2d}{l_1}\right) + l_2\ln\left(\dfrac{2d}{l_2}\right)\right)} \ ,$$

$$\Lambda = \sqrt{k\cos(kl_1)\cos(kl_2)} \ ,$$

$$M_1(\alpha) = \prod_{n=1}^{\infty}\left[1 + \frac{\alpha}{i\gamma_{n1}}\right]e^{\frac{2i\alpha d}{\pi n}} \ ,$$

$$M_2(\alpha) = \prod_{n=1}^{\infty}\left[1 + \frac{\alpha}{i\gamma_{n2}}\right]e^{\frac{i\alpha l_1}{\pi n}} \ ,$$

$$M_3(\alpha) = \prod_{n=1}^{\infty}\left[1 + \frac{\alpha}{i\gamma_{n3}}\right]e^{\frac{i\alpha l_2}{\pi n}} \ .$$

Fields representation. Applying the Liouville's theorem, we arrive at a solution of equation (10) in the following form:

$$U^+(\alpha) = \frac{i\cos(\beta_j h)}{\sqrt{2\pi}M_+(\alpha)}\left[\frac{M_+(\alpha)}{t - i\gamma_j} - \frac{M_+(i\gamma_j)}{\alpha - i\gamma_j}\right]. \qquad (12)$$

Substituting expressions (12) and (8) into representation (10), we find the integral representation of the diffracted field in the form

$$u(x, y) = \frac{1}{\sqrt{2\pi}}\int_{-\infty}^{+\infty}U(\alpha, y)e^{-i\alpha x}d\alpha, \qquad (13)$$

For the field analysis, we represent integral (13) through the series of the residues. For this purpose we deform the integration path into the upper/lower complex half-planes. As a result, the scattered field for each of the regions is written as follows:

I. $x > 0, -d < y < d$:

$$u(x, y) = \frac{\cos(\beta_j h) M_+ (i\gamma_j)}{2d} \times$$

$$\times \sum_{q=0}^{\infty} \frac{\varepsilon_q (-1)^{q+1} M_+ (i\gamma_{q1}) \cos\left(\dfrac{\pi q l_1}{2d}\right) e^{-\gamma_{q1} x}}{\gamma_{q1} (\gamma_{q1} + \gamma_j)} \cdot \cos\left(\frac{\pi q (y - d)}{2d}\right), \tag{14}$$

where $\varepsilon_q = 1/2$, when $q = 0$ and $\varepsilon_q = 1$, when $q \geq 1$;

II. $x < 0, -d < y < h$:

$$u(x, y) = -u_z^{inc}(x, y) + \frac{\cos(\beta_j h) M_+ (i\gamma_j)}{l_1^2} \times$$

$$\times \sum_{q=1}^{\infty} \frac{(-1)^q \pi (2q-1) e^{\gamma_{q2} x}}{2\gamma_{q2} (\gamma_{q2} - \gamma_j) M_+ (i\gamma_{q2})} \cos\left(\frac{\pi (q - 1/2)(y + d)}{l_2}\right); \tag{15}$$

III. $x < 0, h < y < d$:

$$u(x, y) = -u_z^{inc}(x, y) + \frac{\cos(\beta_j h) M_+ (i\gamma_j)}{l_2^2} \times$$

$$\times \sum_{q=1}^{\infty} \frac{(-1)^q \pi (2q-1) e^{\gamma_{q3} x}}{2\gamma_{q3} (\gamma_{q3} - \gamma_j) M_+ (i\gamma_{q3})} \cos\left(\frac{\pi (q - 1/2)(y + d)}{l_1}\right). \tag{16}$$

Numerical analysis. Numerical calculations of the total displacement field are represented for the layer in Fig. 1 for two different positions of the defect: $h = 3d/4$ and $h = d/4$.
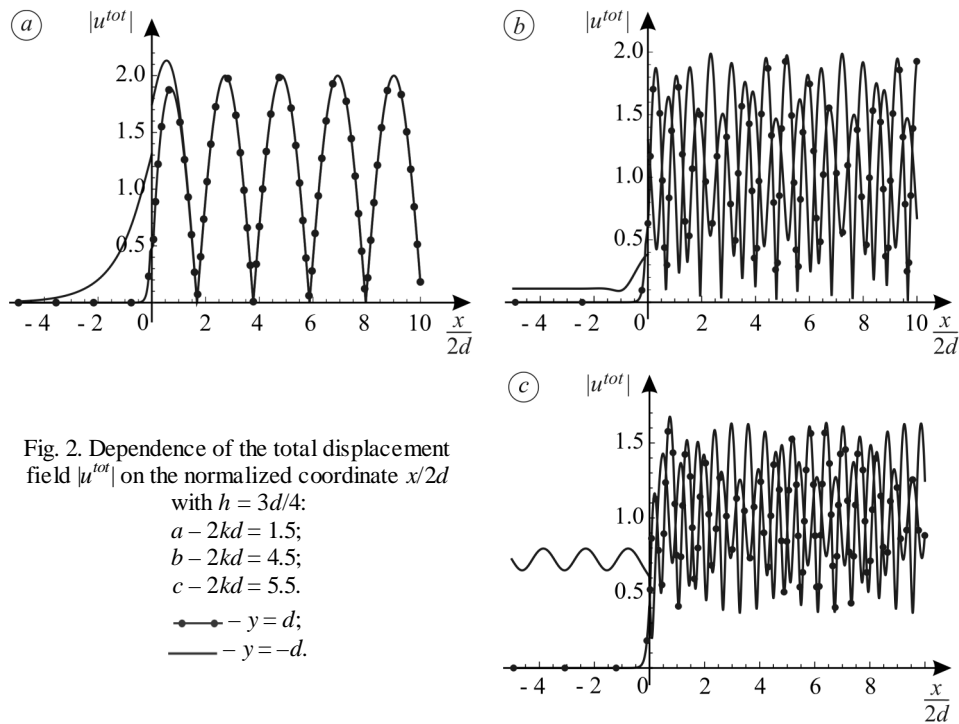
The defect is irradiated by the normal SH-wave (1) with number $j = 0$ of the unit amplitude. The dimensionless thickness of the plate is equal to $2kd$.

Case 1: $h = 3d/4$. Under such condition, all the modes are evanescent in the region $x < 0, h < y < d$, if $0 < 2kd < 2\pi$. In the region $x < 0, -d < y < h$ all the modes are evanescent if $0 < 2kd < 4\pi/7$. In this region the first propagating mode appears if $4\pi/7 < 2kd < 12\pi/7$ and two propagating modes appear if $12\pi/7 < 2kd < 2\pi$.

Case 2: $h = d/4$. In this case all the modes are evanescent in the region $x < 0$, $h < y < d$, if $0 < 2kd < 4\pi/3$. The first propagating mode in this region is formed, if $4\pi/3 < 2kd < 2\pi$. In the region $x < 0$, $-d < y < h$ if $0 < 2kd < 4\pi/5$ all modes are evanescent, and only one propagating mode appears if $4\pi/5 < 2kd < 2\pi$.
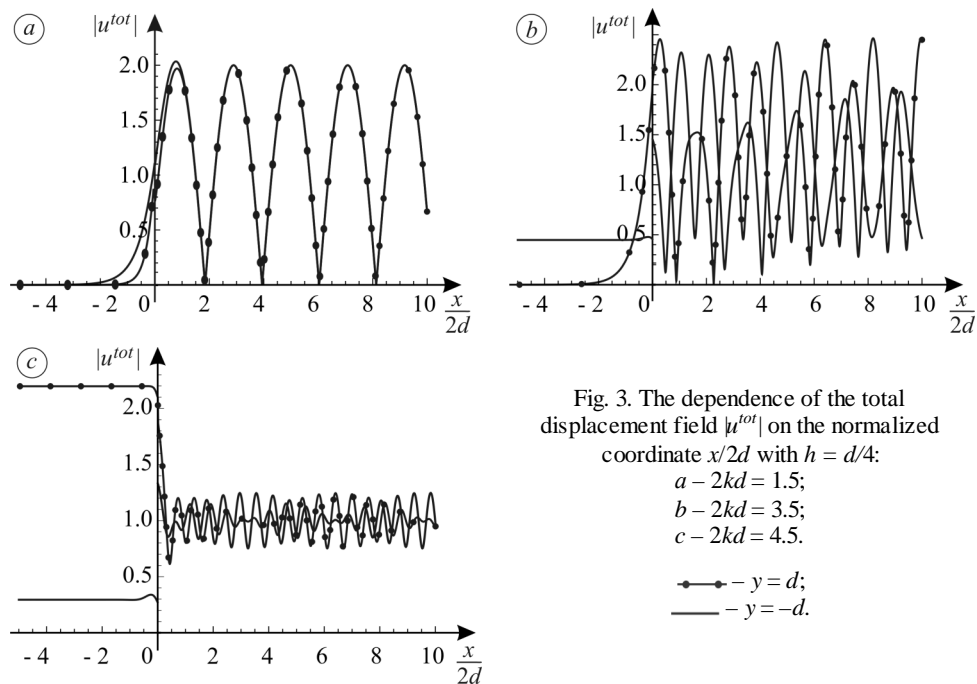
In Figs. 2 and 3 the total displacement fields $\left|u^{tot}\right| = \left|u^{tot}(x/(2d), y = \pm d)\right|$ are shown at the layer surfaces $P(y = \pm d)$: defect $\Gamma(h = 3d/4)$ (see Fig. 2) and defect $\Gamma(h = d/4)$ (see Fig. 3).

Here, taking into account the exponential nature of the damping of summands (14) –(16), no more than five terms were used for the calculations.

a $|u^{tot}|$

2.0
1.5
1.0
0.5

-4 -2 0 2 4 6 8 10 $\dfrac{x}{2d}$

b $|u^{tot}|$

2.0
1.5
1.0
0.5

-4 -2 0 2 4 6 8 10 $\dfrac{x}{2d}$

c $|u^{tot}|$

1.5
1.0
0.5

-4 -2 0 2 4 6 8 $\dfrac{x}{2d}$

Fig. 2. Dependence of the total displacement
field $|u^{tot}|$ on the normalized coordinate $x/2d$
with $h = 3d/4$:
$a - 2kd = 1.5$;
$b - 2kd = 4.5$;
$c - 2kd = 5.5$.
•————• $- y = d$;
———— $- y = -d$.

From Fig. 2a we observe, that in the region $x < 0$ the total field decays to zero on the layer surfaces $y = \pm d$. The speed of the decaying on the surface $y = d$ is higher, than on the surface $y = -d$. This happens because the waveguide area above the inclusion is narrower than the one below. If $x > 0$, the dependence $|u^{tot}|$ on the dimensionless parameter $x/2d$ is oscillatory in its nature. The module of the complex amplitude of the oscillation on the layer surfaces for $y = -d$ and for $y = d$ is different, if $x/(2d) < 1$; and this amplitude is twice as large as the amplitude of the primary normal mode $u_z^{inc}(x, y)$. That is, the oscillations in the incident and reflected waves occur in a phase. With the increase of thickness up to $2kd = 4.5$ (see Fig. 2b), that is equivalent increase of the sounding frequency we see that in the region $x < 0$, $y = d$ the total field $|u^{tot}|$ saves an exponentially decreasing behavior. Here, in the region above of the inclusion, all the modes are evanescent. In the region below the inclusion, one propagating mode is formed. On the surface $x < 0$, $y = -d$ the behavior of $|u^{tot}|$ decreases exponentially to the value 0.25. This corresponds to the amplitude of the scattered mode. Oscillatory behavior of $|u^{tot}|$ is different for the upper and the lower surfaces, if $x > 0$.

With the increase of thickness up to $2kd = 5.5$ (Fig. 2c) in the region above the inclusion all modes are evanescent. On the surface $x < 0$, $y = d$ the behavior $|u^{tot}|$ is exponentially decreased. In the region below the inclusion, two modes are propagating and others are evanescent. In this case, the behavior $|u^{tot}|$ is oscillatory in its nature, if $x < 0$, $y = -d$.

Fig. 3. The dependence of the total displacement field $|u^{tot}|$ on the normalized coordinate $x/2d$ with $h = d/4$:
$a - 2kd = 1.5$;
$b - 2kd = 3.5$;
$c - 2kd = 4.5$.

—•—•— $- y = d$;
———— $- y = -d$.

In Fig. 3 we see the dependences of the total displacement field $|u^{tot}|$ on $y = \pm d$ for $h = d/4$. As follows from Fig. 3 a, $|u^{tot}|$ decays to zero on both surfaces of the layer, if $x < 0$. With the increase of the sounding frequency up to $2kd = 3.5$ one propagating mode in the region $x < 0$, $-d < y < h$ is formed (see Fig. 3b). In this case, on the surface $y = -d$, the value of the amplitude $|u^{tot}| = 0.5$. Here, in the region above the inclusion, all the modes are evanescent.

In the region above and below the inclusion one propagating mode appears, if $2kd = 4.5$ and $x < 0$ (see Fig. 3c); the amplitude $|u^{tot}|$ on the surface $y = d$ is seven times higher than on the surface $y = -d$.

CONCLUSION

Using the Wiener–Hopf technique, we obtain the exact analytical solution of the problem of the diffraction of normal SH-wave on a semi-infinite inclusion, which is located in an elastic plane layer. The influence of the inclusion depth on the distribution of the displacement field, depending on the layer thickness is investigated. It is found that the thickness of the layer and the frequencies of its sounding form intense oscillations of the elastic field on the layer surfaces. The place, where the oscillation start, is an indicator of the defect which can extend to the area where oscillations are absent. The change of the frequency parameter allows the estimation of the defect depth.

1. Nazarchuk, Z., Muravsky, L., Kuryliak, D. To the problem of the subsurface defects detection: theory and experiment *Procedia Structural Integrity* **2019**, 16, 11–18.

2. Thomas, B. P.; Annamala, P. S.; Narayanamurthy, C. S. Investigation of vibration excitation of debonded sandwich structures using time-average digital holography *Appl. Opt.* **2017**, 56, F7–F1.

3. Fomitchov, P.; Wang, L.-S.; Krishnaswamy, S. Advanced image-processing techniques for automatic nondestructive evaluation of adhesively-bonded structures using speckle interferometry *J. Nondestruct. Eval.* **1997**, 16, 215–227.

4. Pouet, B. F.; Krishnaswamy, S. Synchronized reference updating technique for electronic speckle interferometry *J. Nondestruct. Eval.* **1993**, 12, 133–138.

5. Pouet, B. F.; Krishnaswamy, S. Additive-subtractive phase-modulated electronic speckle interferometry: analysis of fringe visibility *Appl. Opt.* **1994**, 33, 6609–6616.

6. Stoykova, E.; Berberova, N.; Kim, Y.; Nazarova, D.; Ivanov, B.; Gotchev, A.; Hong, J.; Kang, H. Dynamic speckle analysis with smoothed intensity-based activity maps *Opt. Lasers Eng.* **2017**, 93, 55–65.

7. Voytko, M. V.; Kutlyk, M. M.; Kuryliak, D. B. The resonant scattering of SH-waves by a finite crack in an elastic layer *Bul.l T. Shevchenko Nat. Univ. Kyiv, Spec. Issue, Ser. Phys. & Math.* **2015**, 51–54.

8. Nazarchuk, Z. T.; Kuryliak, D. B.; Voytko, M. V.; Kulynych, Ya. P. On the interaction of an elastic SH-wave with an interface crack in the perfectly rigid joint of a plate with a half-space *J. Math. Sci.* **2013**, 192, 609–623.

9. Kurylyak, D. B.; Nazarchuk, Z. T.; Voitko, M. V. Analysis of the field of a plane SH-wave scattered by a finite crack on the interface of materials *Mater. Sci.* **2006**, 42, 711–724.

10. Rokhlin, S. I. Resonance phenomena of Lamb waves scattering by a finite crack in a solid layer *J. Acoust. Soc. Am.* **1981**, 69, 922–928.

11. Voytko, M. V.; Kulynych, Ya. P.; Kuryliak, D. B. Resonant scattering of the SH-wave by the interface impedance defect in an elastic layer. In *Proceedings of 16th International Conference on Mathematical Methods in Electromagnetic Theory* (MMET-2016), Lviv, Ukraine, July 5–7, 2016; 264–267.

12. Semkiv, M. Ya.; Zrazhevskyi, H. M.; Matsypura, V. T. Diffraction of normal SH-waves in a waveguide with a crack. *Acoust. Bull.* **2011**, 14, 57–69.

13. Mittra, R.; Lee, S. W. *Analytical Techniques in the Theory of Guided Waves*, New York: Macmillan, 1971.

14. Noble, B. *Methods based on the Wiener–Hopf technique for the solution of partial differential equations* Belfast, Northern Ireland: Pergamon Press, 1958.